**EUMETSAT Satellite Application Facility on Climate Monitoring**

# Algorithm Theoretical Basis Document

# CM SAF Cloud, Albedo, Radiation data record,

# AVHRR-based, Edition 2.1 (CLARA-A2.1)

# Surface Radiation

| | |
|---|---|
| **Surface Incoming Shortwave Radiation** | **CM-11205** |
| **Surface Outgoing Longwave Radiation** | **CM-11255** |
| **Surface Downward Longwave Radiation** | **CM-11265** |

**Document Signature Table**

| | Name | Function | Signature | Date |
|---|---|---|---|---|
| **Author** | Jörg Trentmann | CM SAF scientists | | 05.02.2020 |
| **Author** | | | | |
| **Editor** | Marc Schröder | Co-Science Coordinator | | 26.02.2020 |
| **Approval** | CM SAF Steering Group | | | |
| **Release** | Martin Werscheck | Project Manager | | |

**Distribution List**

| Internal Distribution | |
|---|---|
| **Name** | **No. Copies** |
| DWD Archive | 1 |
| CM SAF Team | 1 |

| External Distribution | | |
|---|---|---|
| **Company** | **Name** | **No. Copies** |
| PUBLIC | | 1 |

**Document Change Record**

| Issue/ Revision | Date | DCN No. | Changed Pages/Paragraphs |
|---|---|---|---|
| 1.2 | 02/07/2012 | SAF/CM/DWD/ATBD/CLARA/RAD | Version for CLARA-A1 Edition |
| 2.0 | 31/03/2015 | SAF/CM/DWD/ATBD/CLARA/RAD | Version presented to PCR 2.2 |
| 2.1 | 26/07/2016 | SAF/CM/DWD/ATBD/CLARA/RAD | Implementation of RIDs from PCR 2.2 |
| 2.2 | 20/05/2016 | SAF/CM/DWD/ATBD/CLARA/RAD | Version presented to DRR-2.2 |
| 2.3 | 31/08/2016 | SAF/CM/DWD/ATBD/CLARA/RAD | Implementation of RIDs from DRR-2.2 |
| 2.4 | 10/02/2020 | SAF/CM/DWD/ATBD/CLARA/RAD | Version for CLARA-A2.1 |
| 2.5 | 09/10/2020 | SAF/CM/DWD/ATBD/CLARA/RAD | Layout revision and barrier free conversion |

**Applicable documents**

| Reference | Title | Code |
|---|---|---|
| AD 1 | CM SAF Product Requirement Document | SAF/CM/DWD/PRD/2.7 |

**Reference documents**

| Reference | Title | Code |
|---|---|---|
| RD 1 | Product User Manual Surface Radiation Products | SAF/CM/DWD/PUM/SFCRAD/ 2.5 |

## Table of Content

## List of Figures

# The EUMETSAT SAF on Climate Monitoring

The importance of climate monitoring with satellites was recognized in 2000 by EUMETSAT Member States when they amended the EUMETSAT Convention to affirm that the EUMETSAT mandate is also to "contribute to the operational monitoring of the climate and the detection of global climatic changes". Following this, EUMETSAT established within its Satellite Application Facility (SAF) network a dedicated centre, the SAF on Climate Monitoring (CM SAF, http://www.cmsaf.eu).

The consortium of CM SAF currently comprises the Deutscher Wetterdienst (DWD) as host institute, and the partners from the Royal Meteorological Institute of Belgium (RMIB), the Finnish Meteorological Institute (FMI), the Royal Meteorological Institute of the Netherlands (KNMI), the Swedish Meteorological and Hydrological Institute (SMHI), the Meteorological Service of Switzerland (MeteoSwiss), and the Meteorological Service of the United Kingdom (UK MetOffice). Since the beginning in 1999, the EUMETSAT Satellite Application Facility on Climate Monitoring (CM SAF) has developed and will continue to develop capabilities for a sustained generation and provision of Climate Data Records (CDR's) derived from operational meteorological satellites.

In particular the generation of long-term data sets is pursued. The ultimate aim is to make the resulting data sets suitable for the analysis of climate variability and potentially the detection of climate trends. CM SAF works in close collaboration with the EUMETSAT Central Facility and liaises with other satellite operators to advance the availability, quality and usability of Fundamental Climate Data Records (FCDRs) as defined by the Global Climate Observing System (GCOS). As a major task the CM SAF utilizes FCDRs to produce records of Essential Climate Variables (ECVs) as defined by GCOS. Thematically, the focus of CM SAF is on ECVs associated with the global energy and water cycle.

Another essential task of CM SAF is to produce data sets that can serve applications related to the new Global Framework of Climate Services initiated by the WMO World Climate Conference-3 in 2009. CM SAF is supporting climate services at national meteorological and hydrological services (NMHSs) with long-term data records but also with data sets produced close to real time that can be used to prepare monthly/annual updates of the state of the climate. Both types of products together allow for a consistent description of mean values, anomalies, variability and potential trends for the chosen ECVs. CM SAF ECV data sets also serve the improvement of climate models both at global and regional scale.

As an essential partner in the related international frameworks, in particular WMO SCOPE-CM (Sustained COordinated Processing of Environmental satellite data for Climate Monitoring), the CM SAF - together with the EUMETSAT Central Facility, assumes the role as main implementer of EUMETSAT's commitments in support to global climate monitoring. This is achieved through:

- Application of highest standards and guidelines as lined out by GCOS for the satellite data processing,

- Processing of satellite data within a true international collaboration benefiting from developments at international level and pollinating the partnership with own ideas and standards,

- Intensive validation and improvement of the CM SAF climate data records,

- Taking a major role in data set assessments performed by research organisations such as WCRP. This role provides the CM SAF with deep contacts to research organizations that form a substantial user group for the CM SAF CDRs,

- Maintaining and providing an operational and sustained infrastructure that can serve the community within the transition of mature CDR products from the research community into operational environments.

A catalogue of all available CM SAF products is accessible via the CM SAF webpage, www.cmsaf.eu/. Here, detailed information about product ordering, add-on tools, sample programs and documentation is provided.

# 1   Introduction

This CM SAF Algorithm Theoretical Basis Document (ATBD) provides information on the processing algorithm implemented for the retrieval of surface radiation parameters from the AVHRR Global Area Coverage (GAC) data. For the shortwave surface radiation the same algorithm is applied as used in the operational surface radiation processing chain. For the retrieval of the longwave surface radiation the algorithm is based on cloud information derived from satellite, reanalysis data, and topographic information.

More information on the basic accuracy requirements are defined in the product requirements document [AD 1]. The CLARA-A2.1 surface radiation data set contains multiple parameters:

Surface Incoming Shortwave Radiation [CM-11205, Section 2.1.1],

Surface Downward Longwave Radiation [CM-11265, Section 2.2.1],

Surface Outgoing Longwave Radiation [CM-11255, Section 2.2.2],

# 2   Retrieval Algorithms of the GAC Surface Radiation Products

In the following the retrieval algorithms used to generate the surface radiation products in the CM SAF CLARA data set will be described. The retrieval of the shortwave surface radiation products (SIS, SNS) is presented in Section 2.1, Section 2.2 presents the algorithms used to derive the longwave surface radiation data sets (SDL, SOL).

## 2.1   Shortwave Surface Radiation

The retrieval algorithm of the surface shortwave radiation (i.e., the surface radiation in the wavelength region between 200 nm and 4000 nm) used for the processing of the AVHRR GAC data is based on the algorithm used in the operational CM SAF chain [RD 1].

The underlying fundamental assumption of retrieving the surface solar irradiance from satellite observations is that the reflected radiance, as measured by the satellite instrument, is related to the broadband atmospheric transmission, T. From the atmospheric transmission the surface incoming solar radiation, SIS, can be derived:

$$SIS = E_0 \cos(\Theta_0) \, T \tag{1}$$

where $E_0$ is the incoming solar flux at the top-of-the-atmosphere ($E_0$ = 1361 W/m$^2$) and $\Theta_0$ the solar zenith angle.

### 2.1.1   SIS Algorithm

The algorithm used here to derive SIS from the AVHRR GAC data set is based on the application of a look-up-table to derive the atmospheric transmission and the surface incoming solar radiation *Pinker and Laszlo, 1992*. The details of the algorithm are given in *Mueller et al.*, 2009]. Here, the basic layout and the fundamental assumptions of the algorithm are presented.

The solar surface irradiance is mainly determined by the solar zenith angle, the cloud coverage, the vertically-integrated water vapour and the aerosol optical depth.

The solar zenith angle (SZA) is determined by the rotation of the Earth, the tilting of the Earth axis and their movement around the sun; the SZA can be accurately calculated. While satellite-based information on the integrated water vapour is available from microwave instruments (e.g., the ATOVS package), these instruments / satellite channels are not available from the AVHRR GAC data set. Also no suitable data set of the aerosol optical depth is available from the AVHRR GAC data. For these two parameters, external data sources have to be consulted

to calculate the transmissivity and the surface solar incoming radiation. The main information that is used from the AVHRR GAC satellite data is the information on cloud coverage.

The retrieval algorithm used to derive the surface incoming solar radiation consists of two steps. First, the full spectral information of the satellite instrument is used to derive information on cloud coverage for each pixel using the Nowcasting SAF (SAFNWC) software. In case, no cloud is detected (i.e., the satellite pixel is considered '*cloud-free*'), the surface solar irradiance is calculated by radiative transfer modelling using information on the integrated water vapour and the aerosol optical depth from auxiliary sources without the use of additional satellite observations. In the case the cloud retrieval algorithm detects the presence of a cloud (i.e., the pixel is classified by the SAF NWC software either as 'cloud-contaminated' or as 'fully cloudy'), the pixel is considered '*cloudy*' and the atmospheric transmissivity and subsequently the surface solar irradiance is derived using the method described in Section 2.1.1.2.

### 2.1.1.1  Cloud-free conditions

The calculation of the surface solar irradiance under cloud-free conditions does not require any additional information from satellite, but is performed using the clear-sky Mesoscale Atmospheric Global Irradiance Code (MAGIC, https://gnu-magic.sourceforge.net/). Figure 2-1 presents the flow-chart of the calculation of the surface incoming solar radiation under clear-sky conditions using MAGIC.
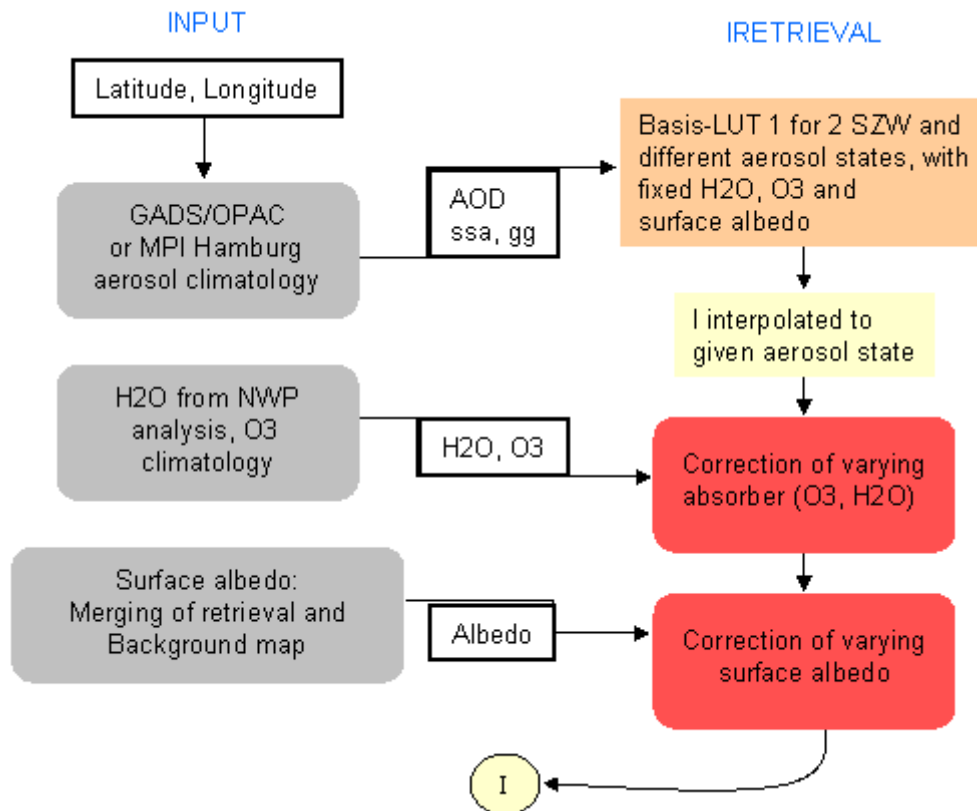
**Figure 2-1:** Flow-chart of the calculation of the surface incoming solar radiation under clear-sky conditions. The required input data is shown on the left side of the diagram, the right part represents the calculation of the surface solar irradiance using the MAGIC clear-sky model. The figure is taken from RW Mueller et al. [2009]. For the SARAH data set, an adjusted version of the GADS / OPAC aerosol climatology has been used (see text for more details).

### 2.1.1.1.1 Auxiliary data

As input parameters, aerosol information (i.e., aerosol optical depth, single scattering albedo, backscattering coefficient), vertically-integrated water vapour and ozone, as well as the surface albedo are required.

#### 2.1.1.1.1.1 Aerosol

For the aerosol information, a modified-version of the monthly mean aerosol fields from the GADS/OPAC climatology [*Hess et al.*, 1998] has been used. Based on the study of *Mueller et al.* [2015] we reduced the maximum AOD values of the original GADS/OPAC climatology to account for the detection of thick aerosol clouds by the cloud retrieval algorithm.

#### 2.1.1.1.1.2 Water vapour and ozon

The integrated water vapour is taken from the ERA-Interim Reanalysis [*Dee et al.*, 2011]; the vertical ozone column, which has a negligible impact on the calculated global radiation, has been set constant to 335 DU.
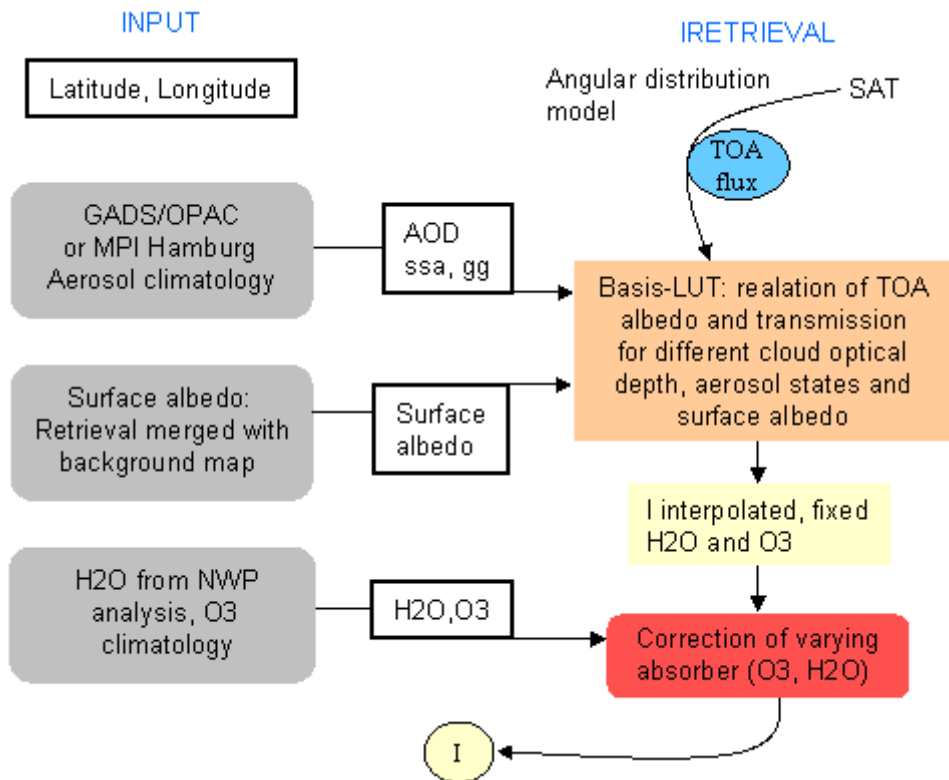
**Figure 2-2:** Diagram of the calculation of the surface solar incoming radiation under cloudy conditions. The required input data is shown on the left side of the diagram, the right part represents the calculation of the surface solar irradiance using the look-up tables for the TOA albedo. The figure is taken from[RW Mueller et al., 2009]. For the SARAH data set, an adjusted version of the GADS / OPAC aerosol climatology has been used (see text for more details).

### 2.1.1.1.1.3 *Surface albedo*

The surface albedo information is calculated based on the spatial distribution of 20 surface types. The Surface and Atmospheric Radiation Budget (SARB) working group, part of the Clouds and the Earth's Radiant Energy System (CERES) mission, provides global digital information on land cover based on scene types from the International Geosphere/Biosphere Programme (IGBP) on a 1/6 deg grid (https://ceres.larc.nasa.gov/data/general-product-info/). Using the broadband albedo for each surface type, a constant global surface albedo map is generated (see Figure 2-3). The use of the temporally constant surface albedo map implies that changes in the surface albedo due to snow and sea ice coverage are not considered in the calculation of the clear sky surface radiation. However, since the impact of the surface albedo on the incoming solar radiation is only moderate, no substantial degradation of the accuracy are expected under clear sky conditions.

This auxiliary information is used in the MAGIC clear-sky solar radiation transfer code to derive the surface solar irradiance when clouds are absent.
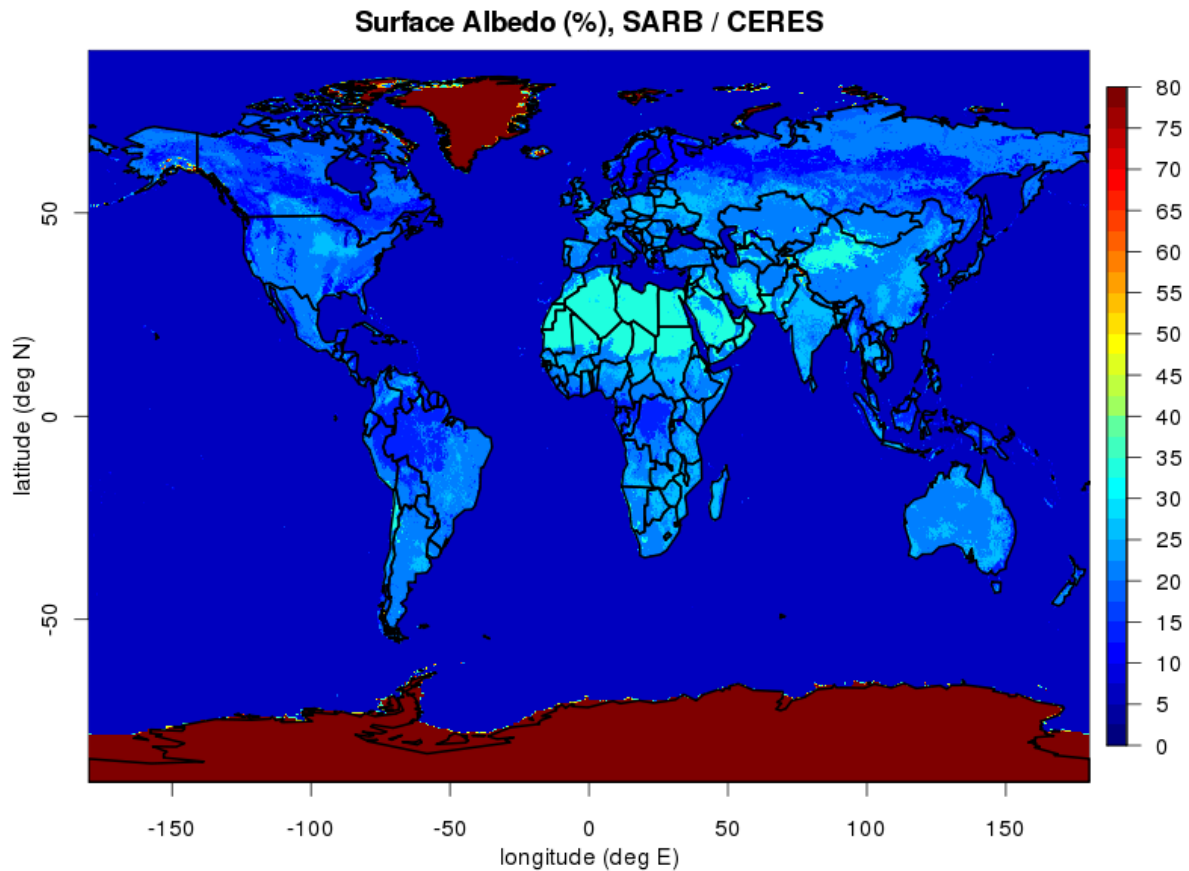
**Figure 2-3:** Spatial distribution of the surface albedo used in the calculation of the clear-sky surface radiation.

### 2.1.1.1.2 The MAGIC clear-sky model

Look-up tables form the core of the MAGIC clear-sky model. They have been pre-calculated for several aerosol optical depths and types, 2 sun zenith angles (0 and 60 degree) with fixed values of surface albedo (0.2), integrated water vapour column (15 mm) and ozone (345 DU) using the RTM model libRadtran [*Mayer and Kylling*, 2005].

To calculate the surface solar radiation for the current atmospheric state (i.e., SZA, water vapour, ozone, surface albedo) correction formulas are applied that consider the difference between the reference value of the parameter (i.e., the value used to derive the look-up-table) and the current value of the parameter. The sensitivity of the clear-sky surface irradiance to the surface albedo is small, i.e., a change of the surface albedo by a factor of 2 (e.g., from 0.2 to 0.4) induces only a 2% change on the surface downwelling clear-sky irradiance [*Mueller et al.*, 2009, Figure 2-4]. The Modified Lambert-Beer (MLB) function is used to derive the dependency of the surface solar radiation from the solar zenith angle based on only 2 pre-calculated solar-zenith angles [*R W Mueller et al.*, 2004]. These optimisations reduce the number of required radiation transfer calculations substantially by a factor of 10.000 compared to 'traditional' look-up table approaches without any loss in the accuracy. The computational efficiency of the algorithm makes it perfectly suited for the satellite retrieval of the surface solar

radiation under clear-sky conditions. No additional information (e.g., the top-of-the-atmosphere reflectance) is used from the satellite measurement.

### 2.1.1.2 Cloudy Condition

Under cloudy conditions (i.e., the pixel is classified as 'cloud-contaminated' or 'fully clouded' by the Nowcasting SAF (SAFNWC) software) a different approach is taken to derive the surface solar radiation. Figure 2-2 presents the diagram of the retrieval of the surface solar incoming radiation under cloudy conditions, which follows the ideas of [*PINKER and LASZLO*, 1992]. The auxiliary input data is identical to the input data used to calculate the clear-sky surface radiation, i.e., surface albedo, vertically-integrated water vapour and ozone, and aerosol information. In addition to this auxiliary input data, also satellite data is used to derive the surface radiation under cloudy conditions.

#### 2.1.1.2.1 Broad-band ToA albedo

The algorithm requires the satellite-derived top-of-the-atmosphere broadband albedo in the shortwave spectral region as input parameter (see Figure 2-2). However, this quantity is not measured directly by the AVHRR instrument, but has to be inferred from measurements in the two visible channels. As a first step, the calculation of the broadband reflectance is conducted based on the measurements of the reflectance in the two visible channels of the AVHRR instruments (see Figure 2-4) following [*Hucek and Jacobowitz*, 1995]. The derived broadband reflectance for each pixel is then transferred to broadband fluxes using the bidirectional reflectance distribution function (BRDF, also termed Angular Dependence Model (ADM)) derived for ERBE [*Suttles et al.*, 1986].

#### 2.1.1.2.2 Look-up tables

The broadband top-of-the-atmosphere albedo is used in a look-up-table approach to derive the atmospheric transmissivity and, subsequently, the surface solar radiation. In addition to the clear-sky approach, under cloudy conditions, also cloud information (in this case the cloud optical depth) has to be taken into account when generating the look-up-tables. To retrieve the relationship between the atmospheric transmissivity and the top-of-the-atmosphere albedo from the look-up-tables, the information on the aerosol optical properties and the surface albedo is taken from the auxiliary data. Based on the measured top-of-the-atmosphere albedo, the corresponding atmospheric transmissivity is extracted from the look-up-tables. As for the clear-sky case, the look-up tables for the cloudy case have been generated for fixed values of vertically-integrated water vapour and ozone. The required correction of the atmospheric transmissivity due to the contribution of these two atmospheric absorbers are applied subsequently (see *Mueller et al.* [2009]).
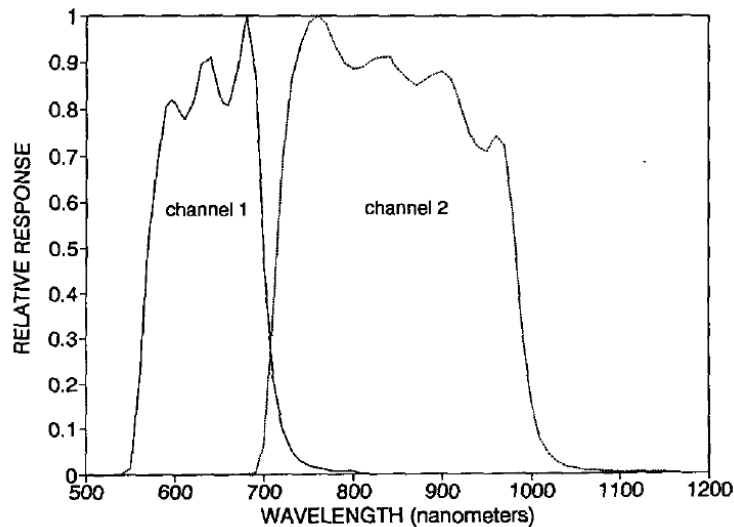
**Figure 2-4:** NOAA 9 AVHRR spectral response functions for the visible (channel 1) and the near-infrared (channel 2) detectors. Figure taken from [Hucek and Jacobowitz, 1995]

In the case of thin clouds over snow-covered surfaces, the use of the constant surface albedo information can lead to an underestimation of the atmospheric transmissivity and subsequently an underestimation of the surface solar radiation. The underestimation of surface solar radiation is correlated to the difference between the actual surface albedo and the assumed climatological value. These differences are expected to be largest under conditions with snow-covered surfaces and, in particular, in the presence of sea ice. It is likely that the accuracy of the CLARA SIS data set will not meet the target accuracy under these conditions.

Based on the retrieved atmospheric transmissivity, the surface solar irradiance is calculated using Equation 1 for each satellite pixel.

### 2.1.1.3  Calculation of gridded averages

The CM SAF CLARA SIS data set generated from the AVHRR satellite measurements is generated and provided on a regular lon-lat grid with a grid point spacing of 0.25° as daily and monthly means. To generate this data from the satellite observations, the information from the satellite retrieval (clear-sky and cloudy-sky solar surface radiation) for each pixel is remapped to a regular lon-lat grid with a spatial resolution of 0.05° using the nearest-neighbour remapping. This resolution is comparable to the spatial resolution of the AVHRR instrument, so no spatial or temporal averaging is performed in this step.

In the next step, the daily mean is calculated following the method by [*MOSER and RASCHKE*, 1984]:

$$I_{dm} = I_{clr,dm} * \frac{\sum I_i}{\sum I_i^{clr}}$$
(2)

here $I_{dm}$ is the daily mean of the surface solar irradiance, $I_{clr,dm}$ is the daily mean of the clear sky surface solar irradiance, $I_i$ is the retrieved surface radiation from the satellite retrieval and $I_i^{clr}$ is the clear-sky surface solar radiation that corresponds to $I_i$. $I_i^{clr}$ is calculated for each satellite pixel during the processing of the satellite data using the MAGIC clear-sky radiation transfer model. The daily mean of the clear-sky surface solar irradiance, $I_{clr,dm}$, is calculated on the 0.05° grid using the MAGIC radiation transfer model. This method to calculate the daily means of the surface radiation substantially reduces the error introduced due to the limited number of observations per pixel per day [*MOSER and RASCHKE*, 1984].

The daily mean surface radiation on the 0.25°-grid is obtained by averaging the corresponding 25 high-resolution grid boxes. To limit the uncertainty of the calculation of the daily averages due to limited number of observations, all daily mean values of the surface solar irradiance that are based on less than 20 observations on the 0.25°-grid are set to missing value.

The monthly mean data of the surface solar irradiance are calculated as averages from the daily mean values. Only those grid boxes are considered that have more than 20 valid daily means of the surface solar radiation. The remaining grid boxes are considered missing data.

The determination of the exact number of the required pixels in each grid box to derive a meaningful daily average and the number of valid daily means to derive a meaningful monthly average needs further investigations. Based on the validation with surface observations (see validation report) the assumed values (20 observations to derive a daily average, 20 daily averages to derive a monthly average) are shown to ensure a quality of the surface irradiance data set in line with the accuracy requirements. It can be expected that these numbers differ depending on season and region. Projects to further evaluate the impact of the number of observations to derive daily and monthly averages from polar-orbiting satellite observations are under way, but have not yet been finalized to be included in the generation of the CLARA SIS data set.

To account for the known inaccuracy of the surface solar irradiance data record under conditions of snow-covered surface, the corresponding grid points have been set to missing data on the daily and the monthly mean data files. To identify the critical grid points the difference between the monthly mean CLARA-A2.1 SAL data record and the surface albedo used in the processing of the SIS data record has been calculated for the full time series. All grid points with a difference in the surface albedo exceeding 35 % have been set to missing data in the final SIS data record. The same holds for all polar pixels.

#### 2.1.1.4  Known Limitations and their Implications

Known limitations and shortcomings of this algorithm to derive the surface solar irradiance:

- The application of the temporally-constant SARB/CERES surface albedo map limits the quality of the data set in regions with varying surface albedo, i.e., in Canada, Alaska, Russia, Scandinavia, and regions with sea ice, during the times when the surface albedo is greatly different from the value assumed in the SARB/CERES albedo map. Even though the impact of this effect has been reduced by masking out the corresponding grid points, however it cannot be completely excluded that the accuracy of the CM SAF CLARA A2 SIS data record in snow-covered areas is outside the target accuracy.

- The algorithm requires broadband solar fluxes at the top-of-the-atmosphere to retrieve the atmospheric transmissivity and subsequently the surface solar radiation. The conversion of the satellite-observed radiances at two wavelengths into broadband solar fluxes requires assumptions on the spectral responses of the satellite channels and the bidirectional reflectance distribution function (BRDF), which can introduce large uncertainty into the satellite retrieval under cloudy conditions.

- The algorithm depends on the ability of the cloud-detection software to detect clouds. Misclassification of pixels by the cloud-detection algorithm enhances the uncertainty of the retrieved surface solar radiation.

- The application of monthly climatological aerosol information limits the accuracy of the data set, especially in regions with high interannual and sub-monthly aerosol variability, e.g., desert regions.

The mentioned limitations will be addresses and improved in future versions of the CM SAF CLARA surface solar radiation data set.

### 2.2  Longwave Surface Radiation Products

This section describes the algorithms to derive the surface longwave radiation products of the CM SAF CLARA data set: The surface downwelling longwave radiation (SDL), the surface outgoing longwave radiation (SOL).

The longwave surface radiation budget is decoupled from the visible and infra-red radiation at the top-of-the-atmosphere [*Ellingson*, 1995], which limits the suitability of the AVHRR GAC data to retrieve the longwave surface radiation components.

The surface downwelling longwave radiation is, under cloud-free conditions, mainly determined by the temperature and water vapour in the lowest kilometre of the atmosphere [*Ohmura*, 2001]. Under cloudy conditions, the height of the cloud base determines the surface downwelling longwave radiation. In both cases, the AVHRR satellite signal alone does not contain enough relevant information to retrieve the surface longwave downwelling radiation within sufficient accuracy.

The surface outgoing longwave radiation is dominated by the surface temperature, which can, under cloud-free conditions, be derived from the AVHRR satellite observations. No information on the surface temperature, and hence the surface outgoing longwave radiation, is present in the satellite measurements under cloudy conditions.

To overcome this fundamental limitation, data from the ERA-Interim data set is used to generate the CM SAF CLARA surface longwave radiation data set. The ERA-Interim data set is generated at the spectral T255 horizontal resolution, corresponding to approximately 79 km spacing on a reduced Gaussian grid [*Dee et al.*, 2011]. To reduce spin-up effects of the reanalysis model, the monthly means of the surface longwave radiation data based on the 12-to-24 h forecasts are used.

The information on the cloud fraction from the CM SAF CLARA CFC data set and additional topographic information is used to provide the high spatial resolution of the CM SAF CLARA surface longwave radiation data sets.

### 2.2.1 SDL Algorithm

The CM SAF algorithm to derive the surface downwelling longwave (SDL) radiation from the AVHRR GAC data set is based on the monthly mean surface downwelling longwave radiation data from the ERA-Interim data set. The CM SAF CLARA cloud fraction (CFC) data set and high-resolution topographic information are used to generate the CM SAF CLARA SDL data set on the global 0.25° grid. The CM SAF CLARA CFC data set is only used to improve the fine scale structure of the ERA-Interim SDL data set; the values of the SDL are scaled such that the SDL values are contained on the ERA Interim resolution.

#### 2.2.1.1 Calculation of the Cloud Correction Factor

In a preparatory step, the sensitivity of the surface downwelling longwave radiation to cloud coverage is determined from the ERA-Interim data set. The cloud correction factor (CCF) is defined as the ratio of the difference between the clear-sky and all-sky surface longwave downwelling radiation to the cloud fraction:

$$CCF = \frac{\Delta SDL}{CFC_{ERA}} = \frac{SDL_{allsky} - SDL_{clr}}{CFC_{ERA}}$$

(3)

The cloud correction factor describes the sensitivity of the surface downwelling longwave radiation to changes in the cloud fraction. The CCF is determined from the ERA-Interim monthly mean data by linear regression between $\Delta SDL$ and $CFC$ for each grid box. The calculation of the regression is conducted separately for each month resulting in a CCF data set for each month of the year based on the 31 years of ERA-Interim data.

All grid boxes with a mean total cloud fraction of more than 20 % and mean $\Delta SDL$ below 3% of SDL are set to zero. In these grid boxes (only in tropical regions), the impact of cloud coverage on the surface downwelling longwave radiation is negligible. The cloud correction factor is derived from the linear regression for grid boxes that exhibit a CFC variability of more than 10 % and for grid boxes with a correlation coefficient between $\Delta SDL$ and $CFC$ above 0.6. For the remaining grid boxes, CCF is extrapolated from neighbouring grid boxes. Figure 2-5 shows the temporally averaged cloud correction factor derived from the 31 year-long ERA-Interim data set.

In the tropical regions, clouds have no impact on the surface downwelling longwave radiation, i.e., the differences of the monthly means of the clear-sky and the all-sky surface downwelling longwave radiation is close to zero, even though cloud coverage is larger than 0. In these regions, the large water vapour content in the lowest atmospheric layer is responsible for most of the downwelling longwave radiation. The impact of clouds on the surface longwave downwelling radiation is largest over the Southern Oceans, especially over the Pacific, where clouds can add more than 100 W/m$^2$ to the clear-sky surface longwave radiation. Low clouds have the largest impact on the surface downwelling longwave radiation; improved detection of low clouds from satellite observations or improved description of low clouds in reanalysis data sets would help to reduce the uncertainties in the SDL.
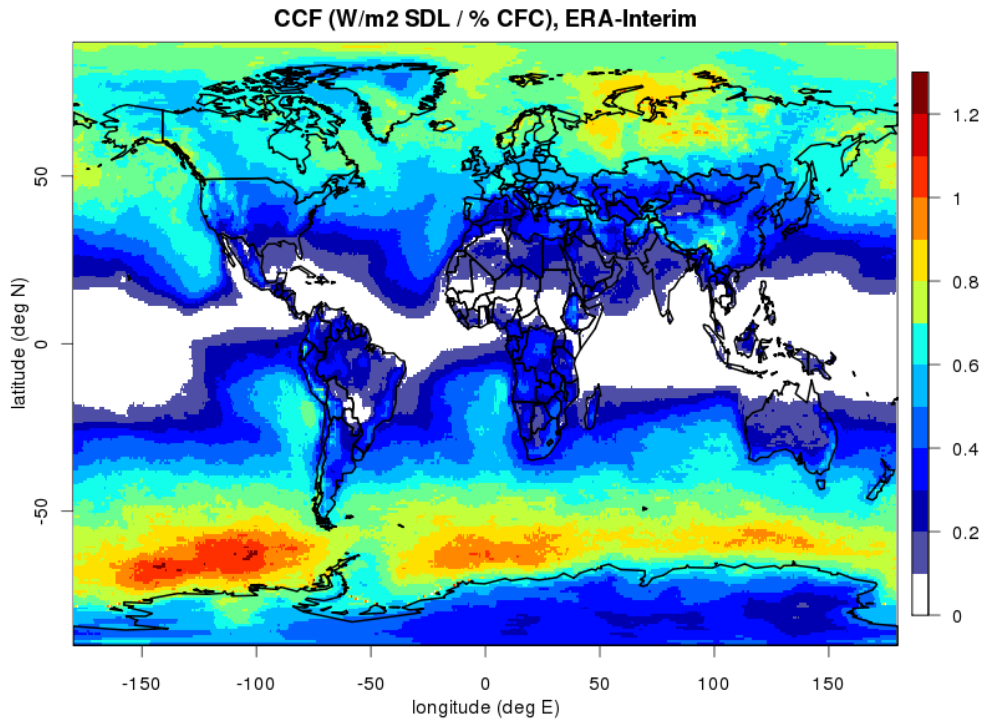
**Figure 2-5:** Temporal average of the cloud correction factor derived from the ERA-Interim data set.

## 2.2.1.2  Calculation of SDL

The surface downwelling longwave radiation from the AVHRR GAC data set is calculated from the monthly mean of the clear-sky surface downwelling longwave radiation derived from ERA-Interim and the cloud correction term, i.e., the *CCF* multiplied with the cloud cover derived from the CM SAF CLARA CFC data set:

$$SDL_{GAC} = SDL_{clr} + CFC_{GAC} * CCF = SDL_{clr} + CFC_{GAC} * \frac{\Delta SDL}{CFC_{ERA}} \qquad (4)$$

here $SDL_{clr}$ denotes the monthly mean clear-sky surface downwelling longwave radiation from ERA-Interim and $CFC_{GAC}$ is the cloud fraction from the CM SAF CLARA data set. By the application of the cloud correction using the CLARA CFC data set the spatial resolution of the data is substantially improved and corresponds to the spatial resolution of the CM SAF CLARA CFC data set. To ensure the conservation of the absolute values from the ERA-Interim data the $SDL_{GAC}$ data is rescaled after this step to reproduce the SDL data from ERA-Interim on the coarse ERA-Interim grid.

Topography substantially modifies the surface longwave downwelling radiation, because of the change in near-surface temperature induced by changes in altitude. Based on observations, [*Wild et al.*, 1995] found that the surface downwelling longwave radiation decreases on average by 2.8 W/m$^2$ per 100 m in elevation. To account for this effect when generating the CM SAF CLARA SDL data set, the Global Land One-km Base Elevation Project (GLOBE) database has been used to calculate the topography on the 0.25° global grid. The GLOBE data set is a global 1-km gridded, quality-controlled Digital Elevation Model (DEM) accessible from the National Geophysical Data Centre at NOAA (http://www.ngdc.noaa.gov/mgg/topo/globe.html). Using the topography information from the ERA-Interim data set, the surface downwelling longwave radiation ($SDL_{GAC}$) has been corrected according to [*Wild et al.*, 1995] to account for the differences in the surface elevation between the two grids The conservation of the surface downwelling longwave radiation on the original ERA-Interim grid is taken into account during the topographic correction by rescaling the high-resolution SDL data to match the SDL on the ERA-Interim grid resolution.

The CM SAF CLARA data set of the surface downwelling longwave radiation is globally available as monthly means from January 1982 to June 2019 with a grid point distance of 0.25°.

### 2.2.1.3   Known limitations

Known limitations and shortcomings of this algorithm to derive the surface downwelling longwave radiation:

- The cloud correction factor (CCF) is determined on a monthly basis by linear regression using ERA-Interim data between 1979 and 2010. By using linear regression to determine CCF, Equation 4 is only valid in an 'average' sense and no interannual variability is considered. For a given year and month the cloud correction of the surface downwelling longwave radiation is (slightly) different to the climatological correction factor for this months. This introduces some uncertainties into the calculation of the CM SAF GAC SDL data set.

- The topography correction of the surface downwelling longwave radiation is based on measurements obtained in the European Alpine region [*Marty et al.*, 2002; *Wild et al.*, 1995]. By analysing the differences between ERA-Interim-derived SDL and global surface observations from the Baseline Surface Radiation Network (BSRN), no improved topographic correction could be determined based on the available observations (Sebastian Limbach, pers. comm.). Dedicated surface observations of the altitudinal dependence of the surface downwelling longwave radiation are required to improve the topographic correction term for the surface downwelling longwave radiation for the global scale. The application of one constant value for the topographic

correction in the calculation of the CM SAF GAC SDL data set is a limitation, which introduces uncertainty.

These limitations will be addressed in future versions of the CM SAF CLARA SDL data set.

## 2.2.2  SOL Algorithm

The surface outgoing longwave radiation (SOL) is primarily determined by the surface temperature and the emissivity of the surface. In the longwave spectral region, the emissivity of the Earth surface is close to unity, resulting in a very small contribution of the reflected surface downwelling longwave radiation to the surface outgoing longwave radiation.

The ability to retrieve the surface outgoing longwave radiation from satellite observations alone is limited by the ability to retrieve the surface temperature with high accuracy. Direct retrieval of the surface temperature from satellite using VIS / IR channels is fundamentally restricted to clear-sky conditions. The high sensitivity of the surface outgoing longwave radiation to the surface temperature (SOL is proportional to $T^4_{srf.}$) results in large uncertainties in the outgoing longwave radiation even under perfect conditions.

Here, we use ERA-Interim data to generate the CM SAF CLARA data set of the surface outgoing longwave radiation. To prepare the CM SAF CLARA data set on the global 0.25° grid, the ERA-Interim data is corrected to account for differences in the terrain elevation and the emissivity between the ERA-Interim grid and the CM SAF CLARA grid.

As a first step, the surface temperature that corresponds to the monthly mean surface outgoing longwave radiation from ERA-Interim is calculated:

$$T_{srf} = \sqrt[4]{\frac{SOL_{ERA}}{\varepsilon \cdot \sigma}} \qquad (5)$$

where $SOL_{ERA}$ is the monthly mean surface outgoing longwave radiation from ERA-Interim, $\varepsilon$ is the emissivity of the ERA-Interim grid box, and $\sigma$ is the Stefan-Boltzman constant ($\sigma$ = 5.67 $10^8$ Wm$^{-2}$ K$^{-4}$).

The surface emissivity on the ERA-Interim grid is based on land cover types provided by the Global Land Cover 2000 (GLC2000) and Global Land Cover Characteristics (GLCC) data bases. Both data sets are derived from analysis of satellite observations and provide the data

at a spatial resolution of 1 km. The GLC2000 data set is mainly based on observations from the VEGETATION instrument onboard the SPOT 4 satellite and covers most of the globe, expect Antarctica [*Bartholomé and Belward*, 2005]; the GLCC data is based on AVHRR measurements [*Loveland et al.*, 2000]. Here, the GLCC is used in regions where GLC2000 information is not available. The land cover types are converted to land type classes and the broadband emissivity is calculated based on the data given in *Wilber et al.* [1999] (See Figure 2-6). The emissivity derived on the original resolution of the land type data are then averaged onto the ERA-Interim grid.
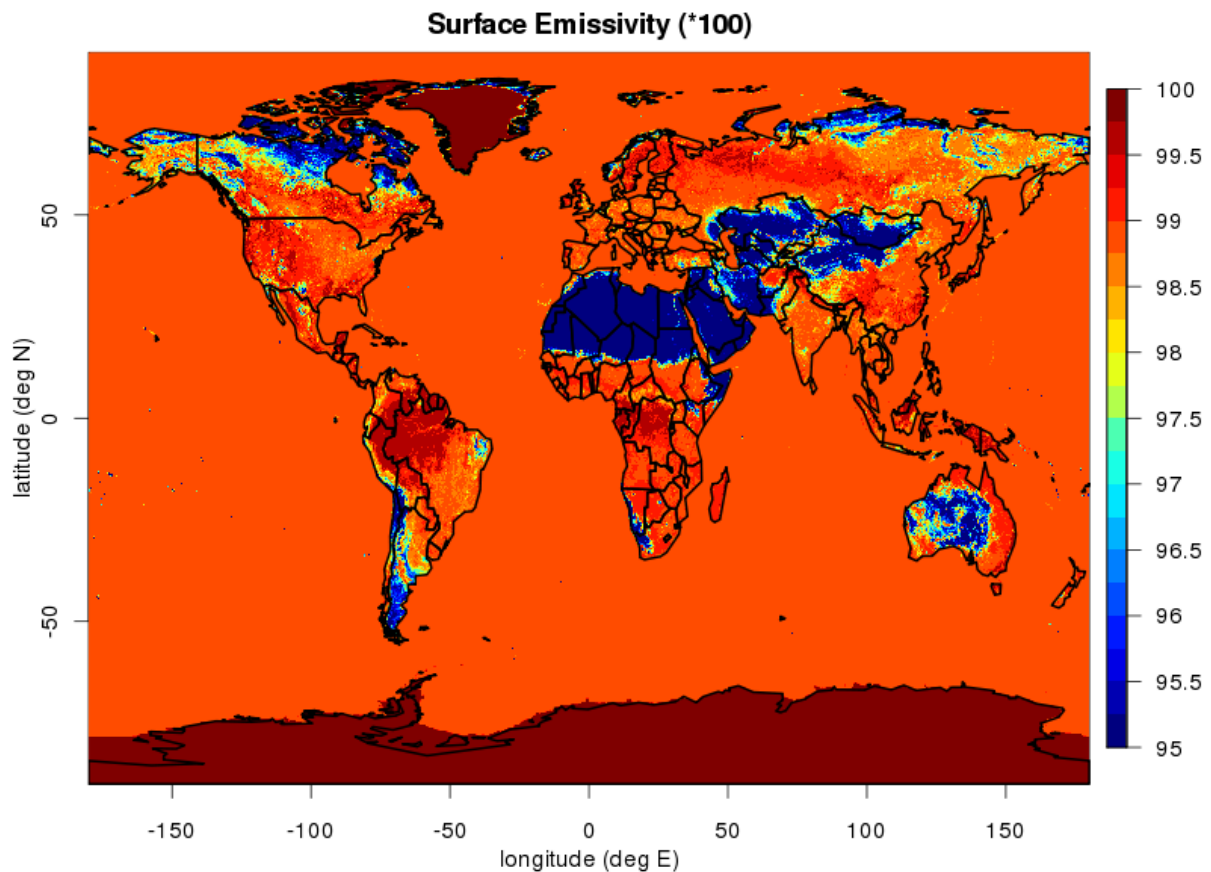


**Figure 2-6:** Surface Emissivity Map derived from land cover types.

The SOL-consistent surface temperature from ERA-Interim is adjusted to account for differences between the terrain elevation on the ERA-Interim grid and the elevation on the global 0.25°-grid by applying the dry-adiabatic temperature gradient of $\Delta T = -9.81$ K / km:

$$\Delta T_{srf} = \Delta h * \Delta T \tag{6}$$

where Δh is the difference in terrain elevation between the 0.25° GAC grid and the ERA-Interim grid in kilometres. The surface outgoing longwave radiation on the global 0.25° grid can then be calculated:

$$SOL = \varepsilon {}^*\sigma {}^*(T_{srf} + \Delta T_{srf})^4 \tag{7}$$

in the calculation of the SOL data set on the global 0.25° grid, it is ensured that the SOL values on the ERA-Interim grid are conserved. The surface outgoing longwave radiation is positively defined in the CM SAF CLARA SOL data set.

### 2.2.2.1 Known limitations

Here is a list of limitations of the SOL data set:

- The topographic correction of the SOL data from ERA-Interim is based on the assumption that the representative monthly mean surface temperature is modified with the dry-adiabatic temperature gradient as a function of elevation. This assumption needs to be verified and introduces some uncertainty in the current data set.
- The emissivity used to derive the surface temperature that corresponds to the monthly mean surface outgoing longwave radiation from ERA-Interim is derived from land type classes and predefined emissivity. In ERA-Interim, the surface emissivity also depends on additional parameters, e.g., soil moisture. Hence, the calculated corresponding surface temperature is slightly different to the one used within ERA-Interim, which introduces some uncertainty in the topographic correction of the SOL ERA-Interim data. The impact on the CM SAF CLARA SOL data set is considered marginal.

# 3 References

Bartholomé, E., and A. S. Belward (2005), GLC2000: a new approach to global land cover mapping from Earth observation data, *International Journal of Remote Sensing*, *26*(9), 1959-1977, doi:10.1080/01431160412331291297.

Dee, D., et al. (2011), The ERA-Interim reanalysis: configuration and performance of the data assimilation system, *Quarterly Journal of the Royal Meteorological Society*, *137*(656), 553-597, doi:DOI 10.1002/qj.828.

Ellingson, R. G. (1995), SURFACE LONGWAVE FLUXES FROM SATELLITE-OBSERVATIONS - A CRITICAL-REVIEW, *Remote Sensing of Environment*, *51*(1), 89-97, doi:10.1016/0034-4257(94)00067-w.

Hess, M., P. Koepke, and I. Schult (1998), Optical properties of aerosols and clouds: The software package OPAC, *Bulletin of the American Meteorological Society*, *79*(5), 831-844, doi:10.1175/1520-0477(1998)079<0831:opoaac>2.0.co;2.

Hucek, R., and H. Jacobowitz (1995), IMPACT OF SCENE DEPENDENCE ON AVHRR ALBEDO MODELS, *Journal of Atmospheric and Oceanic Technology*, *12*(4), 697-711, doi:10.1175/1520-0426(1995)012<0697:iosdoa>2.0.co;2.

Loveland, T. R., B. C. Reed, J. F. Brown, D. O. Ohlen, Z. Zhu, L. Yang, and J. W. Merchant (2000), Development of a global land cover characteristics database and IGBP DISCover from 1 km AVHRR data, *International Journal of Remote Sensing*, *21*(6-7), 1303-1330, doi:10.1080/014311600210191.

Marty, C., R. Philipona, C. Fröhlich, and A. Ohmura (2002), Altitude dependence of surface radiation fluxes and cloud forcing in the alps: results fromn the alpine surface radiation budget network, *Theoretical and Applied Climatology*, *72*, 137-155.

Mayer, B., and A. Kylling (2005), Technical note: The libRadtran software package for radiative transfer calculations - description and examples of use, *Atmospheric Chemistry and Physics*, *5*, 1855-1877.

MOSER, W., and E. RASCHKE (1984), INCIDENT SOLAR-RADIATION OVER EUROPE ESTIMATED FROM METEOSAT DATA, *Journal of Climate and Applied Meteorology*, *23*(1), 166-170.

Mueller, R., C. Matsoukas, A. Gratzki, H. Behr, and R. Hollmann (2009), The CM-SAF operational scheme for the satellite based retrieval of solar surface irradiance - A LUT based eigenvector hybrid approach, *Remote Sensing of Environment*, *113*(5), 1012-1024, doi:DOI 10.1016/j.rse.2009.01.012.

Mueller, R., U. Pfeifroth, and C. Traeger-Chatterjee (2015), Towards Optimal Aerosol Information for the Retrieval of Solar Surface Radiation Using Heliosat, *Atmosphere*, *6*(7), 863-878, doi:10.3390/atmos6070863.

Mueller, R., and C. Träger-Chatterjee (2014), Brief Accuracy Assessment of Aerosol Climatologies for the Retrieval of Solar Surface Radiation, *Atmosphere*, *5*(4), 959-972, doi:10.3390/atmos5040959.

Mueller, R. W., et al. (2004), Rethinking satellite-based solar irradiance modelling - The SOLIS clear-sky module, *Remote Sensing of Environment*, *91*(2), 160-174, doi:10.1016/j.rse.2004.02.009.

Ohmura, A. (2001), Physical basis for the temperature-based melt-index method, *Journal of Applied Meteorology*, *40*(4), 753-761, doi:10.1175/1520-0450(2001)040<0753:pbfttb>2.0.co;2.

PINKER, R., and I. LASZLO (1992), MODELING SURFACE SOLAR IRRADIANCE FOR SATELLITE APPLICATIONS ON A GLOBAL SCALE, *Journal of Applied Meteorology*, *31*(2), 194-211.

Wild, M., A. Ohmura, H. Gilgen, and E. Roeckner (1995), REGIONAL CLIMATE SIMULATION WITH A HIGH-RESOLUTION GCM - SURFACE RADIATIVE FLUXES, *Climate Dynamics*, *11*(8), 469-486, doi:10.1007/bf00207196.